JOURNAL OF SOLID STATE CHEMISTRY 69, 329–335 (1987)

Crystal Structure of the Red Cesium Molybdenum Bronze, $Cs_{0.33}MoO_3$

P. P. TSAI, J. A. POTENZA, AND M. GREENBLATT

Department of Chemistry, Rutgers, The State University of New Jersey, New Brunswick, New Jersey 08903

Received October 10, 1986; in revised form December 4, 1986

The crystal structure of $Cs_{0.33}MoO_3$ has been determined from single-crystal X-ray diffraction data. $Cs_{0.33}MoO_3$ crystallizes in space group $C2/m$ with $a = 15.862(2)$ Å, $b = 7.728(2)$ Å, $c = 6.4080(7)$ Å, $\beta = 94.37(1)°$, $Z = 12$, and $R_F = 0.033$ for 1746 reflections with $F_o^2 \geq 3\sigma(F_o^2)$. The crystal is isostructural with those of the red molybdenum bronzes $K_{0.33}MoO_3$ and $Tl_{0.33}MoO_3$, but is significantly different from a crystal of the red cesium bronze $Cs_{0.25}MoO_3$. A blue powder, obtained by grinding red single crystals of $Cs_{0.33}MoO_3$, can be indexed on the basis of the cell parameters reported above.

Introduction

The preparation of blue and red cesium molybdenum bronze single crystals has been reported. A blue bronze with the empirical formula $Cs_{0.19}MoO_{2.85}$ was found to be monoclinic with cell constants $a = 19.198(4)$ Å, $b = 5.519(2)$ Å, $c = 12.213(2)$ Å, and $\beta = 119.44(2)°$ (*1*). Small well-shaped crystals of the red cesium molybdenum bronze $Cs_{0.33}MoO_3$ were prepared via electrolysis of molten molybdates (Cs_2MoO_4 (30 mole%) and MoO_3 (70 mole%) at 530°C) by Reid and Watts (*2*). The X-ray crystal structure of this red bronze was determined by Mumme and Watts (*3*); the crystals were reported as monoclinic, space group $P2_1/m$ with cell parameters $a = 6.425(5)$ Å, $b = 7.543(5)$ Å, $c = 8.169(5)$ Å, and $\beta = 96.50(5)°$, and the chemical composition, according to the structure determination, $Cs_{0.25}MoO_3$.

Single-crystal red platelets of a cesium molybdenum bronze of composition $Cs_{0.33}MoO_3$, grown by Greenblatt *et al.* (electrolysis of Cs_2MoO_4 (28 mole%) and MoO_3 (72 mole%) at 550°C), were believed to be the same phase as that reported previously (*2, 3*). However, upon grinding, the crystals turned blue and the powder pattern could not be indexed using the cell parameters reported by Mumme and Watts (*3*). Consequently, it was assumed that a phase transformation had occurred upon grinding (*4*). Crystals of red $Cs_{0.33}MoO_3$, grown by the temperature gradient flux technique, showed identical properties to those grown electrolytically (*5*). Although Mumme and Watts determined lattice parameters of their cesium bronze using the Guinier powder technique, they made no mention of a color change upon grinding. Furthermore, they predicted that the stacking of MoO_6 octahedra in $Cs_{0.25}MoO_3$, compared with the semiconducting red potassium analog $K_{0.33}MoO_3$ (*6*), would

0022-4596/87 $3.00

lead to greater delocalization of the unpaired *d* electrons and possibly metallic conductivity in the former. Subsequent measurement of the temperature dependence of the resistivity of red $Cs_{0.33}MoO_3$ crystals grown either electrolytically or by the gradient flux technique showed semiconducting behavior with a room temperature resistivity of $\rho \sim 10^5$ Ω-cm (*4*); $K_{0.33}MoO_3$ showed similar behavior with ρ (300 K) $\sim 10^4$ Ω-cm (*7, 8*).

Initial X-ray examination of our single crystals of $Cs_{0.33}MoO_3$ revealed a *C*-centered monoclinic lattice (space group *C*2, *Cm*, or *C*2/*m*) with cell parameters significantly different than those reported by Mumme and Watts. To help clarify some of the ambiguities noted above, a single-crystal structure determination of $Cs_{0.33}MoO_3$ was undertaken. We report here the results of that determination.

Experimental

Platelet-shaped crystals of $Cs_{0.33}MoO_3$ were prepared using a temperature gradient flux growth technique (*5*), and a single crystal 0.48 × 0.16 × 0.06 mm was mounted on a glass fiber. Details of the data collection process and structure solution are given in Table I. Diffractometer examination of the reciprocal lattice revealed Laue symmetry 2/*m* and the systematic absence *hkl*, $h + k = 2n + 1$, consistent with the *C*-centered monoclinic space groups, *C*2, *Cm*, and *C*2/*m*. Successful solution and refinement of the structure fixed the space group as *C*2/*m*. Intensity data were collected and corrected for Lorentz, polarization, absorption (empirical), and decay effects.

The structure was solved by a combination of direct methods and difference Fourier techniques. The program MULTAN 82 (*9*) and the "Enraf–Nonius Structure Determination Package" (*10*) were used. Full-matrix least-squares refinement was based on *F* and neutral atom scattering factors were used. Anomalous dispersion corrections were applied to the scattering factors of the Cs, Mo, and O atoms. All atoms were located from an initial *E* map and two successive difference maps. Several cycles of anisotropic refinement led to convergence with $R_F = 0.033$ and $R_{wF} = 0.049$. As a check of the stoichiometry of the crystal, the Cs atom multiplier was refined before the final cycles. The refined value was 0.5039(6), indicating complete

TABLE I

CRYSTAL AND REFINEMENT DATA FOR $Cs_{0.33}MoO_3$

fw	187.80
a, Å	15.862(2)
b, Å	7.728(2)
c, Å	6.4080(7)
β, deg	94.37(1)
V, Å^3	783.2(4)
Space group	*C*2/*m*
Z	12
No. of reflections used to determine cell constants	25 ($19.79 \leq \theta \leq 24.00$)
d calcd, g/cm^3	4.789
λ (Mo*Kα*), Å	0.71073
Monochromator	Graphite
Linear absorption coefficient, cm^{-1}	92.0
Relative transmission factor range	$0.9 \leq T \leq 1$
Diffractometer	Enraf–Nonius CAD-4
Data collection method	θ–2θ
2θ range, deg	4–70
Temperature K	297(1)
Scan range, deg	$1.20 + 0.35 \tan \theta$
Weighting scheme	$w = 4(F_0)^2/[\sigma(F_0)^2]^2$[a]
No. of standard reflections	3
% Variation in standard intensity	±0.2
No. of unique data collected	1774
No. of data used in refinement	1746 ($F_0^2 \geq 3\sigma(F_0^2)$)
Data : parameter ratio	25.3
Final GOF[b]	1.97
Final R_F[c]	0.033
Final R_{wF}[d]	0.049
Systematic absence observed	*hkl*, $h + k = 2n + 1$
Final largest shift/*esd*	0.01
Highest peak in final difference map, *e*/Å^3	2.1

[a] $[\sigma(F_0)^2]^2 = [S^2(C + R^2B) + rF_0^2)^2]/(Lp)^2$, where *S* is the scan rate, *C* is the total integrated peak count, *R* is the ratio of scan to background counting time, *B* is the total background count, and *r* is a factor introduced to downweight intense reflections. For the present structure, $r = 0.04$.

[b] Error in an observation of unit weight, equal to $[\Sigma w(|F_0| - |F_c|)^2/(NO\text{-}NV)]^{1/2}$ where NO is the number of observations and NV is the number of variables in the least-squares refinement.

[c] $R_F = \Sigma||F_0| - |F_c||/\Sigma|F_0|$.

[d] $R_{wF} = [\Sigma w(|F_0| - |F_c|)^2/\Sigma wF_0^2]^{1/2}$.

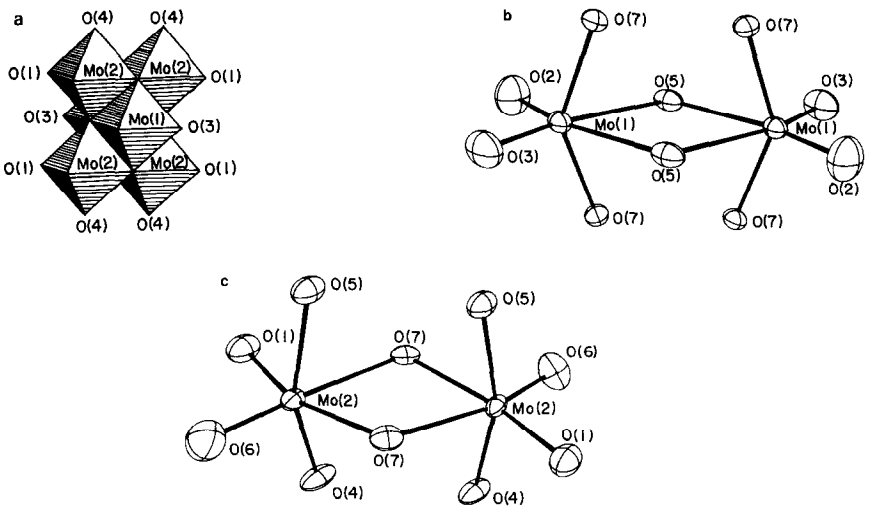

FIG. 1. (a) Idealized basic six Mo cluster unit viewed approximately along [100]. (b) ORTEP drawing of two edge-shared Mo(1) octahedra with atomic numbering scheme. (c) ORTEP drawing of two edge-shared Mo(2) octahedra with atomic numbering scheme.

occupancy of the 4*i* site in *C*2/*m* (multiplier = 0.5) and verifying the stoichiometry as $Cs_{0.33}MoO_3$. A final difference map showed no unusual features; the largest positive peak (2.1 $e/Å^3$) was located 1.60 Å from the Cs atom. Final atomic parameters are given in Table II. Lists of observed and calculated structure factors, and of anisotropic temperature factors, are available as supplementary material.[1]

Results and Discussion

The red cesium molybdenum bronze $Cs_{0.33}MoO_3$ ($CsMo_3O_9$) is isostructural with its potassium and thallium(I) analogs $K_{0.33}MoO_3$ (*6*) and $Tl_{0.33}MoO_3$ (*11*). The basic unit of structure is six edge-sharing molybdenum–oxygen octahedra (Mo_6O_{22} units, Fig. 1a) which corner-share along the *b* and *c* directions to form infinite layers joined by Cs^+ ions. The *b* and *c* cell parameters correspond roughly to the height and width, respectively, of the Mo_6O_{22} units and each is the same to within 0.05 Å in the

TABLE II

FRACTIONAL ATOMIC COORDINATES AND THERMAL PARAMETERS

	x	*y*	*z*	Beq(Å²)[a]
Cs	0.30763(2)	0	0.16941(5)	1.359(5)
Mo(1)	0.11018(2)	0	0.64754(5)	0.570(5)
Mo(2)	0.05334(2)	0.26097(3)	0.27227(4)	0.511(4)
O(1)	0	0.2586(4)	0	0.95(5)
O(2)	0.2059(3)	0	0.5416(6)	1.45(6)
O(3)	0.1345(3)	0	0.9100(6)	1.19(5)
O(4)	0.5352(3)	0	0.2970(5)	0.94(5)
O(5)	0.0368(2)	0	0.3130(5)	0.73(5)
O(6)	0.1560(2)	0.2617(3)	0.2236(4)	1.31(4)
O(7)	0.0745(1)	0.2376(3)	0.5960(4)	0.62(3)

[a] The isotropic equivalent temperature factor Beq is given by $Beq = 4/3 \sum_i \sum_j \beta_{ij} a_i a_j$.

[1] See NAPS document No. 04459 for 9 pages of supplementary material. Order from ASIS/NAPS. Microfiche Publications, P.O. Box 3513, Grand Central Station, New York, NY 10163. Remit in advance $4.00 for microfiche copy or for photocopy, $7.75 up to 20 pages plus $0.30 for each additional page. All orders must be prepaid. Institutions and organizations may order by purchase order. However, there is a billing and handling charge for this service of $15. Foreign orders add $4.50 for postage and handling, for the first 20 pages, and $1.00 for additional 10 pages of material, $1.50 for postage of any microfiche orders.

TABLE III

SELECTED INTERATOMIC DISTANCES (Å) AND BOND STRENGTHS, *s*

Octahedron	Mo(1)	*s*	Mo(1)[a]	Octahedron	Mo(2)	*s*	Mo(2)[a]
–O(2)	1.710(3)	1.78	1.73(5)	–O(1)	1.8802(2)	1.01	1.96(3)
–O(3)	1.697(3)	1.86	1.59(4)	–O(4)	1.8780(5)	1.01	1.96(4)
–O(5)	2.360(2)	0.26	2.16(3)	–O(5)	2.0531(5)	0.59	2.01(7)
–O(5′)	2.364(3)	0.26	2.55(4)	–O(6)	1.682(2)	1.96	1.64(4)
–O(7) × 2	1.943(2)	0.83	1.99(4)	–O(7)	2.084(2)	0.54	2.19(4)
		5.80		–O(7′)	2.262(2)	0.33	2.15(4)
						5.45	
O(2)–O(3)	2.694(4)			O(1)–O(4)	2.693(2)		
O(2)–O(5)	2.956(4)			O(1)–O(5)	2.860(2)		
O(2)–O(7) × 2	2.820(3)			O(1)–O(6)	2.764(2)		
O(3)–O(5)	2.973(4)			O(1)–O(7)	2.931(2)		
O(3)–O(7) × 2	2.835(3)			O(4)–O(6)	2.724(3)		
O(5)–O(5)	2.745(5)			O(4)–O(7)	2.792(3)		
O(5)–O(7) × 2	2.618(2)			O(4)–O(7′)	2.826(2)		
O(5)–O(7) × 2	2.643(3)			O(5)–O(6)	2.857(3)		
O(5)–O(7)	2.618(2)						
O(5)–O(7′)	2.643(3)						
O(6)–O(7)	2.806(3)						
O(7)–O(7′)	2.579(3)						

	Polyhedra			
	Cs	Cs[a]	Mo–Mo	
Cs–O(2)	2.980(3)	2.76(4)	Edge-shared	
–O(3)	3.100(3)	3.34(5)	Mo(1)–Mo(1)	3.8452(5)
–O(6) × 2	3.181(2)	3.07(4)	Mo(1)–Mo(2)	3.2145(3)
–O(6′) × 2	3.207(2)	3.34(4)	Mo(1)–Mo(2′)	3.3559(3)
–O(7) × 2	3.073(2)	3.19(4)	Mo(2)–Mo(2)	3.4833(4)
O(6)–O(6) × 4	3.683(4)		Corner-shared	
O(6)–O(7) × 4	3.922(3)		Mo(2)–Mo(2′)	3.6946(4)
O(7)–O(7)	3.673(3)		Mo(2)–Mo(2″)	3.7603(3)

[a] Distances for $Cs_{0.25}MoO_3$ taken from Ref. (*3*).

three structures. The *a* cell parameter corresponds to the interlayer distance and, as might be expected, increases with the effective ionic radius of the monovalent cation. The charge density of Cs^+ (a = 15.862(2) Å) is smaller than that of K^+ (a = 14.278(8) Å) and Tl^+ (a = 14.537(1) Å); therefore, Mo-containing sheets in the Cs bronze are more loosely held together by the cations than in the K and Tl bronzes.

Selected interatomic distances and bond strengths are listed in Table III while bond angles are given in Table IV. Mo–O bond strengths were calculated using the equation $s = (d/d_0)^{-N}$, where d_0 = 1.882 Å and N = 6.0 are constants taken from the compilations of Brown (*12*); d is the observed interatomic distance. The MoO_6 octahedra are severely distorted, with Mo–O distances ranging from 1.682(2) to 2.364(3) Å. *cis*-O–Mo–O angles range from 71.03(9) to 104.6(1)° while the corresponding *trans* angles vary from 141.9(1) to 167.93(8)°. Judging from the bond strength values, it is probably more appropriate to consider Mo(1) as pseudo-4-coordinate because two

TABLE IV

SELECTED INTERATOMIC ANGLES (DEG)

	cis		*cis*
	Mo–O octahedra		
O(2)–Mo(1)–O(3)	104.6(1)	O(1)–Mo(2)–O(6)	101.63(7)
O(2)–Mo(1)–O(5)	91.8(1)	O(1)–Mo(2)–O(7)	89.59(4)
O(2)–Mo(1)–O(7)	100.87(6) × 2	O(4)–Mo(2)–O(6)	99.7(1)
O(3)–Mo(1)–O(5)	92.6(1)	O(4)–Mo(2)–O(7)	90.88(8)
O(3)–Mo(1)–O(7)	102.13(6) × 2	O(4)–Mo(2)–O(7)	84.3(1)
O(5)–Mo(1)–O(5)	71.03(9)	O(5)–Mo(2)–O(6)	99.32(9)
O(5)–Mo(1)–O(7)	74.99(5) × 2	O(5)–Mo(2)–O(7)	78.50(7)
O(5)–Mo(1)–O(7)	74.23(5) × 2	O(5)–Mo(2)–O(7)	75.37(8)
O(1)–Mo(2)–O(4)	91.5(1)	O(6)–Mo(2)–O(7)	95.76(9)
O(1)–Mo(2)–O(5)	93.2(1)	O(7)–Mo(2)–O(7)	72.68(7)
	trans		*trans*
O(7)–Mo(1)–O(7)	141.9(1)	O(1)–Mo(2)–O(7)	161.77(5)
O(2)–Mo(1)–O(5)	162.8(1)	O(4)–Mo(2)–O(5)	159.0(1)
O(3)–Mo(1)–O(5)	163.7(1)	O(6)–Mo(2)–O(7)	167.93(8)
	Cs–O polyhedra		
O(2)–Cs–O(3)	85.28(8)	O(6)–Cs–O(6)	129.29(3) × 2
O(2)–Cs–O(6)	56.82(5) × 2	O(6)–Cs–O(6)	70.08(7)
O(2)–Cs–O(6)	140.28(4) × 2	O(6)–Cs–O(7)	82.31(5) × 2
O(2)–Cs–O(7)	87.42(5) × 2	O(6)–Cs–O(7)	128.61(5) × 2
O(3)–Cs–O(6)	54.02(5) × 2	O(6)–Cs–O(6)	84.44(6) × 2
O(3)–Cs–O(6)	77.51(6) × 2	O(6)–Cs–O(7)	143.43(5) × 2
O(3)–Cs–O(7)	138.05(3) × 2	O(6)–Cs–O(7)	87.94(5) × 2
O(6)–Cs–O(6)	78.96(7)	O(6)–Cs–O(7)	82.59(6)

of the Mo(1)–O bonds have particularly small s values. If O(5) and O(5′) are assumed not to be bonded to Mo(1), the coordination geometry of Mo(1) is that of a distorted octahedron with two vacant *cis* sites (Fig. 1b). The coordination geometry of Mo(2) (Fig. 1c) is more difficult to describe; here we simply note that Mo(2) forms one Mo–O double bond, two single bonds, and three rather weak bonds with its nearest neighbor O atoms.

The basic unit of six Mo octahedra (Fig. 1a) is closely packed and repulsions between Mo ions are great. This is reflected in the Mo(1)–Mo(1) distance (3.8452(5) Å, Table III) which is much larger than typical edge-shared octahedral Mo–Mo distances and even longer than the corner-shared Mo(2)–Mo(2) distances (3.4833(4) Å) in the present structure. Finally, we note that the intercluster corner-shared Mo–Mo distance (3.7603(3) Å) is slightly larger than that within a cluster (3.6946(4) Å).

The calculated average valence for the Mo sites is 5.56, in good agreement with the value of 5.67 expected from the chemical formula determined from the crystallographic data. Mo valence values can be used to determine the Mo^{5+}/Mo^{6+} charge distribution for each crystallographically distinct site (*13*). This gives $Mo(1)^{6+}_{0.80}Mo(1)^{5+}_{0.20}$ and $Mo(2)^{6+}_{0.45}Mo(2)^{5+}_{0.55}$ for the two molybdenum sites, suggesting that the Mo(2) sites have substantially more d-electrons (85% of those available) than the Mo(1) sites. A similar calculation for the Tl analog yields a value of 83% for the d-electrons on the Mo(2) sites. A comparison of this type with $K_{0.33}MoO_3$ is not possible because of the large coordinate *esd*'s in that structure (*6*).

In these red bronzes, the stoichiometry implies that two electrons are donated to each Mo_6O_{22} cluster. Based on detailed EPR measurements of $K_{0.33}MoO_3$, Bang and Sperlich (*14*) concluded that the d^1 electrons in that structure are delocalized over the six Mo sites in the cluster. Further, their analysis suggested that these electrons are paired and lie in a molecular orbital comprised of Mo $4d_{xy}$ orbitals where x corresponds to the shortest Mo–O distance and y to the crystallographic b direction. Alkali metal vacancies give rise to unpaired d electrons in some clusters and this, in turn, leads to residual paramagnetism and the EPR spectra. Ganne *et al.* (*11*), using this model, interpreted the semiconducting behavior of $Tl_{0.33}MoO_3$ in terms of thermally activated electrons hopping from cluster to cluster via these molecular orbitals. Travaglini and Wachter (*15*) have analyzed the conductivity difference between blue $K_{0.3}MoO_3$, a one-dimensional metallic conductor along b at room temperature, and red $K_{0.33}MoO_3$, a semiconductor along b and c, in terms of differences in $Mod_{t_{2g}}$–Op_{π} overlap along Mo–O–Mo chains. For appropriately short Mo–O distances, large overlap leads to bands and metallic conductivity while longer Mo–O distances, as in $K_{0.33}MoO_3$, yield cluster-

localized orbitals and semiconductor behavior. Because of their structural similarities, similar interpretations should hold for the physical properties of $Cs_{0.33}MoO_3$.

In $Cs_{0.33}MoO_3$, eight oxygen atoms are bonded to each Cs cation: O(2), O(3), and 2 × O(6) from one layer, and 2 × O(6) and 2 × O(7) from the adjacent layer (Fig. 2). The Cs coordination polyhedron, which can be described either as a distorted square antiprism or as a trigonal prism capped on two rectangular faces, is similar to those reported for the K and Tl(I) analogs. In all three structures, the Cs polyhedra are linked via O(6) to form infinite zigzag chains along *b*.

Comparison of the present structure with that of $Cs_{0.25}MoO_3$ reported by Mumme and Watts shows that both structures are closely related. In $Cs_{0.25}MoO_3$, the basic building block is the Mo_6O_{22} cluster, shown in Fig. 3, which can be formed formally from the clusters in Fig. 1a by translation of one Mo(1) unit by $\frac{1}{2}b$. These Mo_6 clusters are linked by edge-sharing along *b* and corner-sharing along *a* to form infinite layers in the (001) plane again joined by Cs^+ ions. The different linking along *b* results in

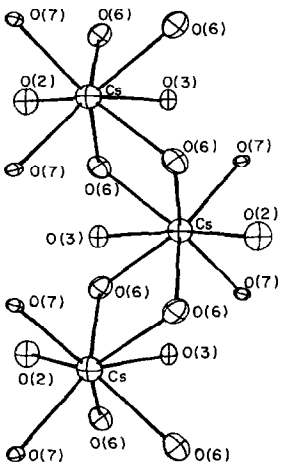

FIG. 2. ORTEP drawing of chain of Cs polyhedra.

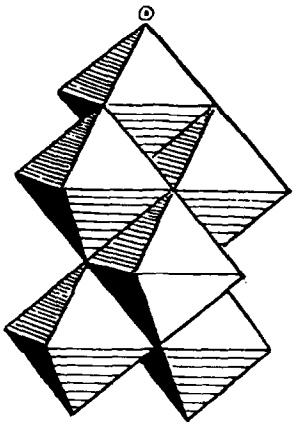

FIG. 3. Idealized basic six Mo cluster unit in $Cs_{0.25}MoO_3$.

significant differences in coordination geometries. As might be expected, larger differences in Mo–O distances are observed for Mo(1) as compared with Mo(2) (Table III) because the environment of Mo(1) changes most from one structure to the other. Indeed, Mo(1) is best described as pseudo-5-coordinate in $Cs_{0.25}MoO_3$ and pseudo-4-coordinate in $Cs_{0.33}MoO_3$. The Cs coordination geometries of both structures are very similar; although there are some significant differences in Cs–O distances (Table III), both structures can be described using the same distorted polyhedra.

Lastly, we note that the X-ray powder diffraction pattern of the blue powder obtained by grinding crystals of red $Cs_{0.33}MoO_3$ can be indexed using the cell parameters reported above, which suggests that no phase change has occurred upon grinding.

Acknowledgments

This work received support from the National Science Foundation—Solid State Chemistry Grant DMR-84-04003—and from the National Institutes of Health—Crystallographic Instrumentation Grant 1510 RR0 1486 01A1.

References

1. L. F. SCHNEEMEYER, S. E. SPENGLER, F. J. DISALVO, J. V. WASZCZAK, AND C. E. RICE, *J. Solid State Chem.* **55,** 158 (1984).
2. A. F. REID AND J. A. WATTS, *J. Solid State Chem.* **1,** 310 (1970).
3. W. G. MUMME AND J. A. WATTS, *J. Solid State Chem.* **2,** 16 (1970).
4. P. STROBEL AND M. GREENBLATT, *J. Solid State Chem.* **36,** 331 (1981).
5. K. V. RAMANUJACHARY, M. GREENBLATT, AND W. H. MCCARROLL, *J. Cryst. Growth* **70,** 476 (1984).
6. N. C. STEPHENSON AND A. D. WADSLEY, *Acta Crystallogr.* **19,** 241 (1965).
7. A. WOLD, W. KUNNMANN, R. J. ARNOTT, AND A. FERRETTI, *Inorg. Chem.* **3,** 545 (1964).
8. G. H. BOUCHARD, JR., J. PERLSTEIN, AND M. J. SIENKO, *Inorg. Chem.* **6,** 1682 (1967).
9. P. MAIN, S. J. FISKE, S. E. HULL, L. LESSINGER, G. GERMAIN, J.-P. DECLERCQ, AND M. M. WOOLFSON, "MULTAN 82: A System of Computer Programs for the Automatic Solution of Crystal Structures from X-ray Diffraction Data," Universities of York, and Louvain (1982).
10. The "Enraf–Nonius Structure Determination Package," Enraf–Nonius, Delft, Holland (1983), was used for data collection, processing, and structure solution.
11. M. GANNE, M. DION, AND A. BOUMAZA, *C. R. Ser. II* **302,** 635 (1986).
12. I. D. BROWN, "Structure and Bonding in Crystals" (M. O'Keefe and A. Navrotsky, Eds.), Vol. II, p. 1, Academic Press, New York (1981).
13. M. GHEDIRA, J. CHENAVAS, AND M. MAREZIO, *J. Solid State Chem.* **57,** 300 (1985).
14. G. BANG AND G. SPERLICH, *Z. Phys. B* **22,** 1 (1975).
15. G. TRAVAGLINI AND P. WACHTER, *Solid State Commun.* **47,** 217 (1983).